INSTRUMENTATION, TESTING AND POTENTIALITIES OF AN INERTIA LOADING MACHINE

by

Raymond Elliott Mesloh

Thesis submitted to the Graduate Faculty of the
Virginia Polytechnic Institute
in candidacy for the degree of

MASTER OF SCIENCE
in
APPLIED MECHANICS

APPROVED:	APPROVED:
Director of Graduate Studies	Head of Department
Dean of Engineering	Major Professor

May 1, 1958

Blacksburg, Virginia

TABLE OF CONTENTS

Page

I. LIST OF FIGURES

Figure | Page

II. NOMENCLATURE

The notation used in this thesis is summarized below:

Symbols	Definition	Units
a	Yoke acceleration	ft/sec^2
a_p	Peak acceleration	ft/sec^2
A_i	Input attenuation	db or %
A_f	Filter attenuation in pass range	db or %
c	Viscous damping coefficient	# sec/in
c_c	Critical damping coefficient	# sec/in
C	Capacitance	mmfd
C_a	Accelerometer capacitance	mmfd
C_t	Shunt capacitance	mmfd
do	Oscilloscope deflection	cm
db	Decibel	
δ	Logarithmic decrement	
E_c	Accelerometer calibrated voltage	mv/g
E_o	Output voltage	mv/g
E_s	Standardized accelerometer voltage	mv/g
fc	Cutoff frequency	cps
fn - ω n	Undamped natural frequency	cps-rad/sec
fnd - ωnd	Damped natural frequency	cps-rad/sec
g	Acceleration of gravity	32.16 ft/sec^2
Gi	Input amplifier gain	

Symbols	Definition	Units
Gv	Oscilloscope vertical gain	mv/cm
k	Spring gradient	#/in
L	Inductance	Henries
$\mathcal{L}$	Laplace transform	
M	Filter derivation	
m	Mass	$\#sec^2/ft$
$r=c/c_c$	Viscous damping ratio	
S	Laplace step function	
s	Laplace function	
t	Time	seconds
T	Pulse duration	seconds
u	Absolute displacement of mass	ft.
X	Displacement of yoke	ft.
y=u - X	Relative displacement	ft.

III. INTRODUCTION

Prediction of the behavior of a structure or system under service conditions has always been the basis of engineering design. During its service life, a structure or system is subjected to many variable forces. When forces vary slowly or with a very low frequency as compared to the natural frequencies of the structure or system, the design may be essentially static. However, when the varying force is of such nature to excite the natural frequencies of the structure or system, consideration must be given to its response to the actual dynamic loading. "Excitation which induces strong transient vibrations is often called shock to distinguish it from the steady-state or forced type of excitation. Naturally, the dividing line between steady-state vibration and shock is somewhat vague and difficult to define with any great exactness. In general, shock will exist when the change in exciting force or displacement is either frequent or sudden."[1]* While prediction of shock loading is difficult, much has been learned by field testing concerning the magnitude and duration of service loads.

Laboratory simulation of shock loading utilizes two basic modes of evaluating the response of a system to shock:[2]

(a) To simulate actual shock conditions imposed on a system and determine whether the system

---

* The numbers in brackets refer to references listed in the bibliography.

can withstand the shock.

(b) To produce shock of various durations and determine the degree of damage to the system.

The most common means of accomplishing these types of shock loading is the inertia loading machine, the most popular ones being the vertical drop tester and the pendulum tester. The shock loading is specified in terms of acceleration produced on the test specimen in terms of peak value, shape and duration of the acceleration time pulse. Shock machines in current use operate on four general principles to obtain their shock motion: (1) centrifugal effects, (2) acceleration by compressed air or explosion of gases, (3) acceleration by steel springs, and (4) impact following acceleration of the test carriage by gravity or compressed air.[3] Most drop testers derive their shock from the impact and either elastic or plastic deformation of their striking surfaces after acceleration by gravity or compressed air.

The magnitude and duration of the shock applied to the test carriage is recorded by measuring the actual acceleration pulse magnitude in relation to time. It is occasionally advantageous to measure the displacement pulse with respect to time.

The drop tester considered in this thesis uses the impact of various shaped wooden blocks with sand, to produce its shock motion, after the test carriage is accelerated by gravity. Measurement of the shock is accomplished by using a piezoelectric accelerometer mounted on the carriage.

IV. REVIEW OF LITERATURE

Most of the shock testing discussed in available literature is being conducted by the Department of the Navy[2,3,4] and the Westinghouse Research Laboratories[5,6]. Nowhere in these articles is discussed or mentioned a drop tester using sand as a stopping medium except in a product bulletin[10] by the Berry Corporation. In this bulletin, the sand drop tester, after which the Applied Mechanics Shock Machine was designed, is discussed with respect to its range of application. Calibration curves for the machine are given with characteristic shock patterns.

It seems that the sand drop tester has given way to more specialized machines using the impact of steel against steel or lead to produce their shock motions. Due to this change of impact surfaces a greater range of peak accelerations may be obtained with more consistant shock patterns. These machines are discussed in detail by J. H. Armstrong in his article[3] on shock testing at the Naval Ordnance Laboratory. An important table is given in this article comparing many of their shock machines as to their acceleration range, pulse duration and size.

Another prominent short duration shock machine is the pendulum type tester discussed in an article by Irwin Vigness[4]. This type tester uses a heavy hammer which hits the bottom or edge of an anvil table on which equipment to be tested is mounted. The range of peak acceleration for this machine depends upon the hammer weight which

may be varied, the arc of swing and the test specimen weight. With this machine, the shock may be repeated at regular intervals of one to several times a minute.

E. G. Fischer of Westinghouse Research Laboratories used this type of pendulum tester in determining the transient response of a laterally vibrating uniform beam. In this test, the ends of the beam were hinged to suitable supports and the supports bolted to the anvil table. The anvil table and thus the beam ends were given a triangular shaped displacement wave with respect to time. Response of the beam was determined from strain gages mounted on the beam. A mathematical solution was presented which corresponded with the experimental results. Operational calculus, mainly the Laplace Transform Integral was used in solving this problem. According to the author, it represents a formalized method of solution and leaves no doubt as to the correct interpretation of unfamiliar transient solutions[1, 5].

A theoretical prediction of elastic impact drop testers and a comparison with actual test performance is given in an article by M. Kornhauser[2]. This article also gives the practical design limitations and discusses in detail the potentialities of this type of high impact tester.

Except for the square wave tester[3], sine wave tester[3] and the machine discussed by Kornhauser[2], the acceleration wave shapes for drop testers are not discussed. However, to simulate actual shock conditions the pulse shapes are important. Salvadori,

in his article[7], presents a criteria for considering the influence of pulse shape, area and duration on a system response. For short duration pulses the peak acceleration and total velocity change are of more importance[7].

V. INVESTIGATION

A. Description of Apparatus

The shock machine* tested and discussed in this thesis is a gravity drop tester deriving its shock motion from the impact of yellow pine blocks in sand. This machine and the electrical equipment used to record the shock pulse is illustrated in Figure 1.

1. Mechanical Details

The carriage is lifted into drop position by means of a 1/4 hp gear motor capable of raising the carriage with a 100# test load. Rubber guide wheels on the lifting frame serve only to insure proper orientation of the carriage for the drop and to constrain the carriage from rocking after impact. The drop is considered as a free fall with only a minimum of interference from the guides.

An enlargement of the carriage shows the face plate, used for bolting test specimens, resting directly on the stiffened rectangular box frame for attaching the impact blocks. (Figure 2) The upper striped frame is used only for lifting the carriage and attaching lead wires. The approximate weight of the carriage assembly is 70# depending upon the number of impact blocks used for the drop. An

---

* This shock machine was built and instrumented for the Applied Mechanics Department at V.P.I. 1958

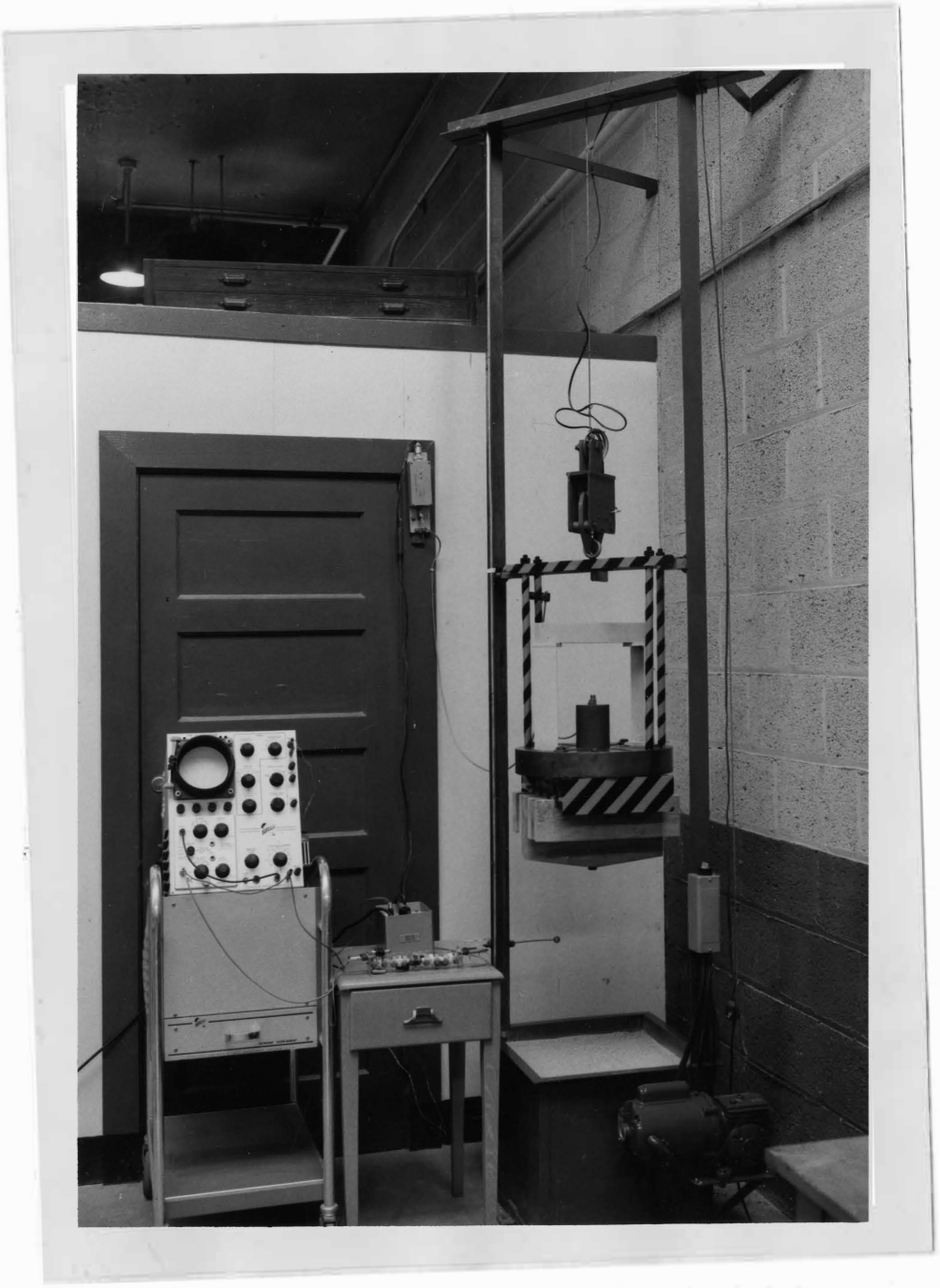

Figure 1. Drop Tester and Electrical Equipment

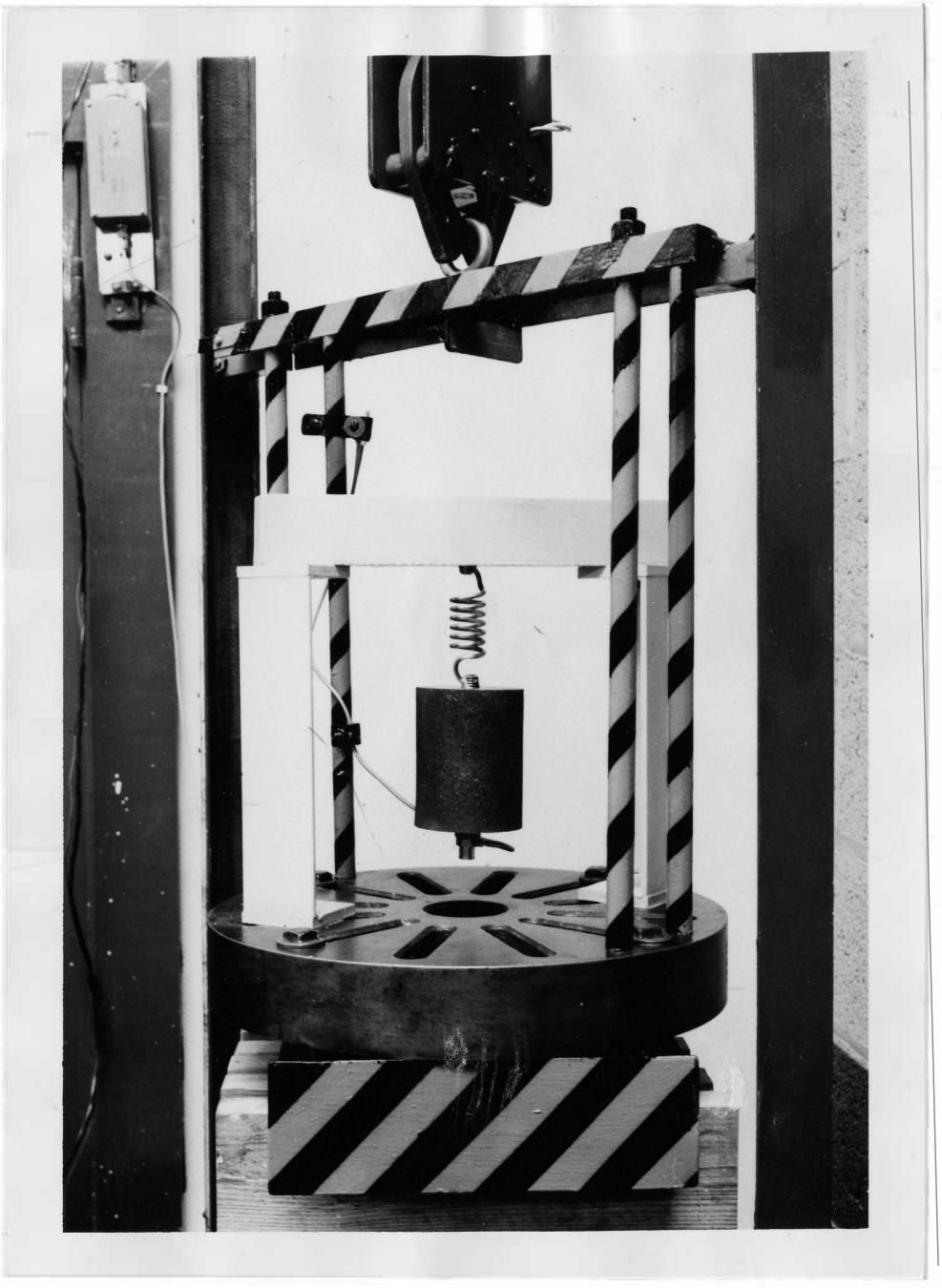

Figure 2. Carriage Details

electrical solenoid release is used for dropping the carriage and is designed so that the weight of the carriage locks the release against accidental opening.

The machine is solidly bolted to a concrete floor with its guide angles plumbed and braced to eliminate excessive vibrations of the machine frame. Its base is filled with 300# of common sand.*

The machine is set up and calibrated to apply a maximum peak acceleration of 170 g's or a maximum dropping height of 54 inches corresponding to a velocity change of 17 ft/sec with 30# of test equipment. With certain modifications** in carriage design and base mounting, 100# of test equipment could be shock loaded with a maximum peak acceleration of 300 g's.

2. Electrical Instrumentation

In the process of shock testing considerable attention must be given to the reliability of the recorded shock in representing that actually present. It is for this reason that the following electrical instrumentation parameters*** were used. Figure 3 represents a single line block diagram of the electrical components and circuit

---

* IX Appendix B Sand Test Data

** VI Discussion of Results-D Recommendations

*** IX Appendix A

used to record the shock pulse.

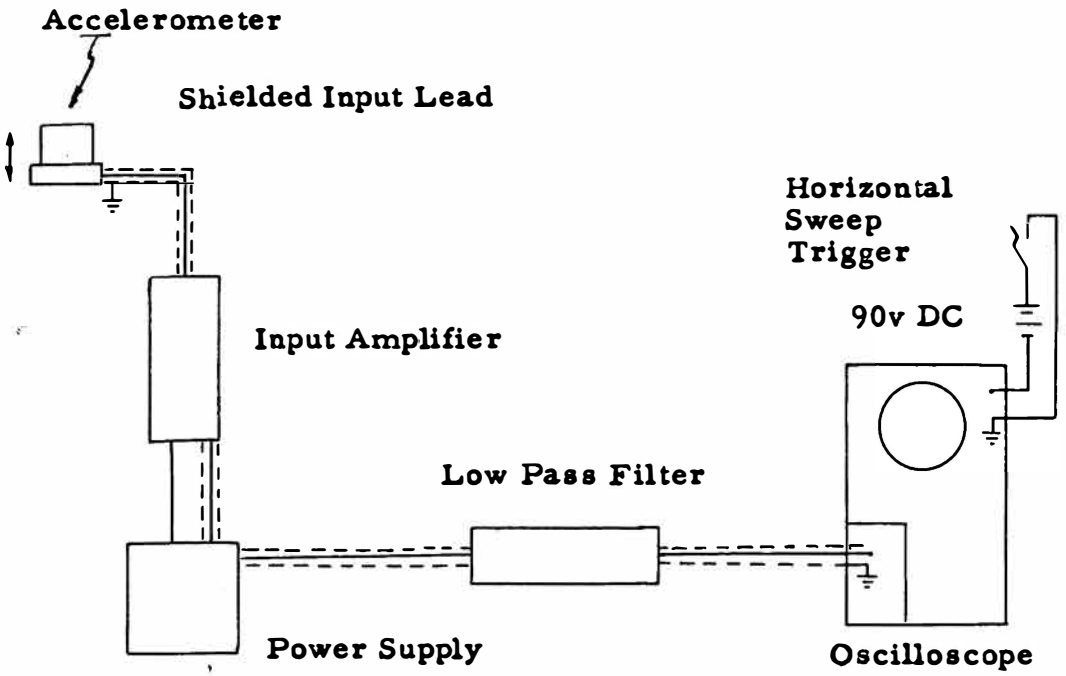

Figure 3. Electrical Instrumentation Block Diagram

Accelerometer

The shock transducer used was a barium titanate accelerometer which represents the ideal laboratory instrument for measuring shock[6]. Its prime objections are easily remedied and out weighed by its advantages.

The accelerometer, being a low output electrical device, requires considerable amplification, thus increasing the noise to signal ratio. Extreme care must be exercised in proper shielding and grounding of all loads to eliminate extraneous noise pickup. Two other objections

are: (1) that shock may excite the accelerometer at its own natural frequency which is above 5000 cps and (2) that the sensitivity or voltage output of the accelerometer increases with frequency above 2500 cps, both of which may be seen from Figure 4. These objections were eliminated by using a low pass filter with a cutoff frequency (fc) of 5000 cps. This frequency was used in order to obtain a linear pass band as large as possible and still eliminate these objections.

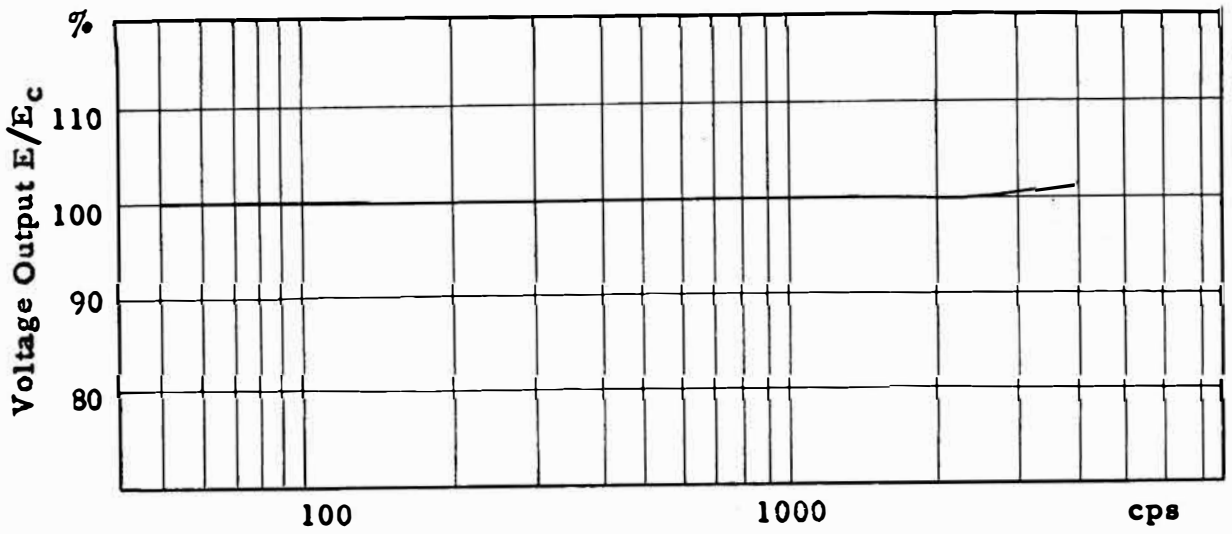

Figure 4. Accelerometer Frequency Response[11]

Advantages of the accelerometer are: (a) its small size and weight make it easy to apply to light test specimens, (b) its flat frequency response to 4000 cps and high sensitivity make it adaptable to measure accelerations over this wide range of frequencies, (c) its output may easily be electrically integrated for velocity or

displacement measurements[8], and (d) due to its sensitivity in one direction it will only measure the component of shock perpendicular to its base.

The piezoelectric accelerometer used in this thesis was calibrated by the manufacturer[11] at 7.0 mv/g RMS (steady-state VTVM Readings) or $7\sqrt{2}$ mv/g for peak shock readings (oscilloscope) over a frequency range of 40 to 4000 cps. Figure 4 represents the per cent voltage output to rated output versus frequency of the pickup used (showing a rising characteristic after 2500 cps). The effect of this rising characteristic is compensated by an increase in filter attenuation at 2000 cps (Figure 5a) producing essentially a flat response to 3000 cps which embraces the expected shock frequency. This filter is shown in Figure 5b.

Input Amplifier and Power Supply

The Input Amplifier[11] powered by the Power Supply is designed for amplification and load matching of high impedance electrical devices. It consists of a three position Gain Switch and Input Selector Switches providing three types of inputs and a Capacitor Decade portion.

The Gain Switch provides amplification positions of 1, 3 and 10 times and is accessible without removing the amplifier cover as is needed with the other switches.

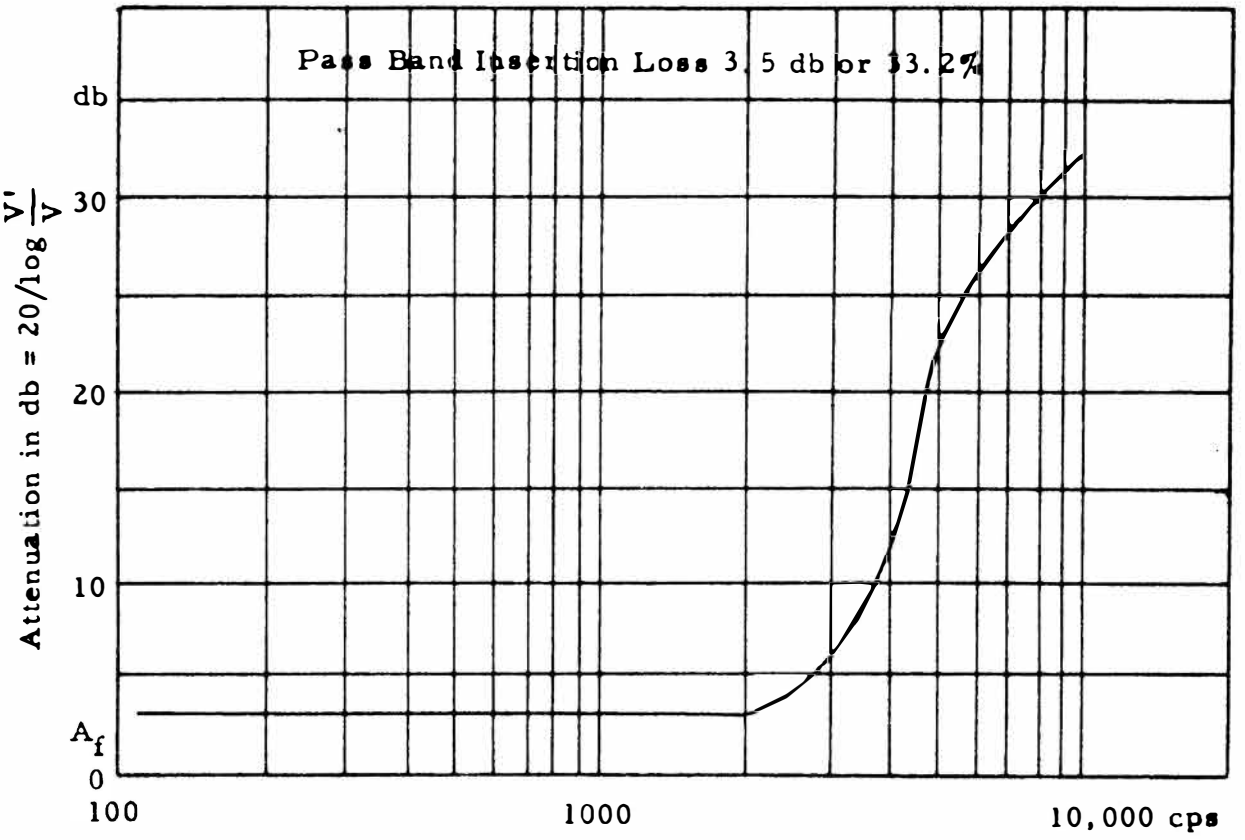

Figure 5a. Low Pass Filter Attenuation Curve

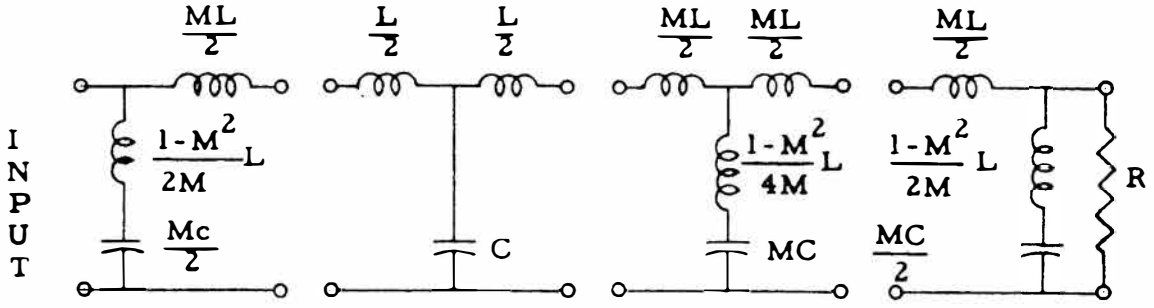

Figure 5b. Low Pass Filter

With the cover removed, the first switch is a three position one marked 1, 2, 3. Position 1 provides 1000 megohms input impedance with no capacitive coupling or DC isolation for use with all piezoelectric and capacitive type devices. Position 2 provides the same input impedance as Positon 1 and a 0.02 mfd coupling capacity for DC isolation. Position 3 provides 22 megohms input impedance and a 0.02 mfd coupling for DC isolation and is recommended for all shock and transient vibration work.

The three decade capacitance portion provides shunt capacitance in 10 mmfd steps to 10,000 mfd across any piezoelectric pickup for standardizing it to any desired level*. Figure 6 shows the variation of output as the shunt capacity is increased.

Low Pass Filter

A low pass filter[4, 9] was incorporated in the circuit for three reasons: (1) to eliminate any resonance of the accelerometer above 5000 cps, (2) to eliminate possible vibration pickup of steel hitting steel which may obliterate the shock pulse and (3) to eliminate pickup of undesirable carriage vibrations.

Its design was based on a cutoff frequency (fc) of 5000 cps and a terminating impedance of 1200 ohms. All values of

---

* See Accelerometer Output Standardization

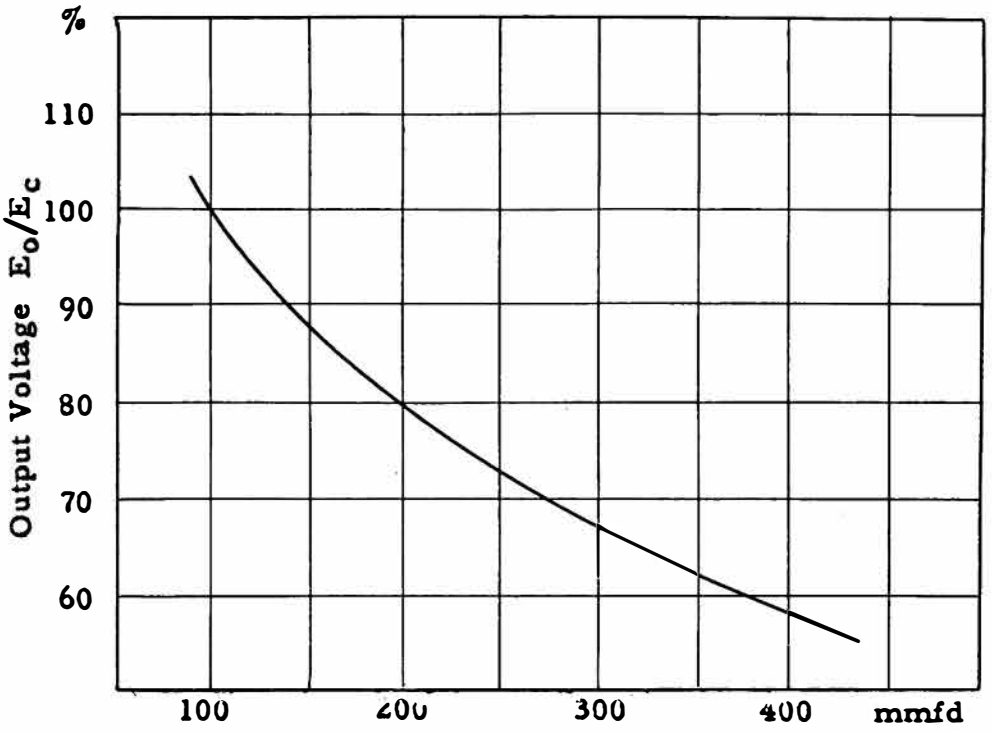

Figure 6. Variation of Accelerometer Output with Capacitive Loading[11]

inductance and capacitance for the filter were calculated in terms of fc and R where

$$L = R/\pi f_c \quad \text{and} \quad C = 1/\pi Rfc \text{ in Figure 5b.}$$

Due to the commercial tolerances of the filter components used, the attenuation curve (Figure 5a) did not have as sharp a cut off or flat pass range as designed but the desired effect was achieved.

The filter attenuation curve was determined by plotting the attenuation in decibels for frequency steps of 100 cps. The attenuation

in decibels for any given frequency was calculated from the equation

$$A = 20 \log V'/V$$

where V'/V is the ratio of voltage delivered to the oscilloscope before insertion of the filter to the voltage after insertion of the filter.

To determine the attenuation of this filter, V' was measured for a constant voltage input to the Input Amplifier. Then the filter was added and V was measured for the same constant voltage thus insuring the same V' for all ranges of frequencies. The input voltage was held near the average level of accelerometer output of 0.5 volts. Figure 7 shows the electrical circuit used for this test.

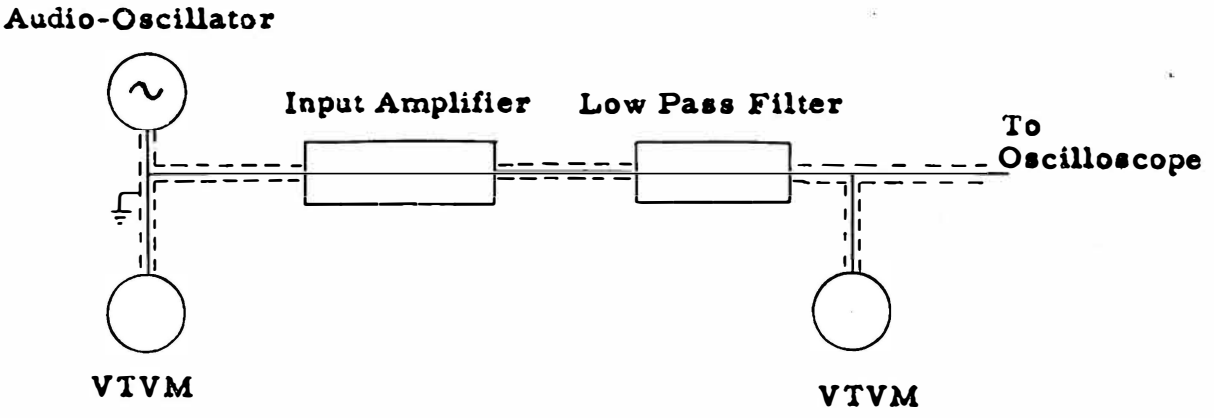

Figure 7. Filter Attenuation Measurement Circuit

Oscilloscope

A camera equipped oscilloscope was used for a visual and permanent record of the shock pulse magnitude and duration. Due

to the versatility of the oscilloscope and precision of the Vertical and Horizontal Deflection Systems, a calibrating wave was not needed to compare the duration or magnitude of the pulse.

Horizontal Sweep Trigger

A micro switch located on the lower part of the left guide angle (Figure 1) was used to trigger the horizontal sweep of the oscilloscope a fraction of a second before the carriage impact.

3. Accelerometer Circuit Standardization

The accelerometer may be illustrated[11] as a zero impedance source in series with a given capacitance C_a representing the internal capacitance of the accelerometer shunted by external capacity (cables, imput, etc.) C_t.

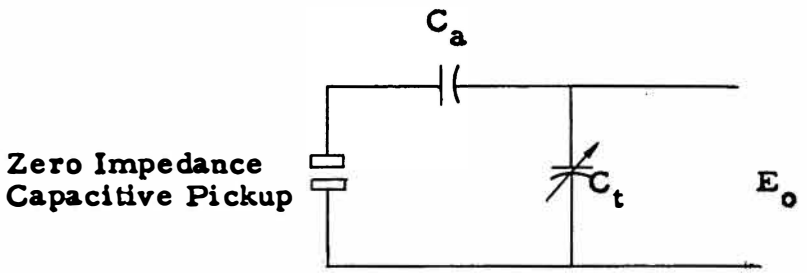

Figure 8. Accelerometer Input Circuit Representation[11]

As may be determined from the circuit, C_a and C_t form a voltage divider with the output voltage Eo varying inversely as C_t. (Figure 6) Thus Eo may be calculated for any capacitive load by the equation:

$$Eo = \frac{E_c (C_a + 100)}{C_a + C_t} \qquad (11)$$

where E_c is the calibrated output voltage at 100 mmfd loading

C_a is the accelerometer capacitance,

and C_t is the capacitance of the input lead and added decade capacitance.

In this thesis an accelerometer of 300 mmfd capacitance calibrated at an E_c of $7\sqrt{2}$ mv/g was shunted with a 220 mmfd input lead and 10 mmfd of the input amplifier giving an Eo equal to 75.5% E_c. Using an input amplifier gain of one, the filter attenuation of 3.5 db or 33.2% reduced the signal input of the oscilloscope to 5.0 mv/g.

Accelerometer Standardization and Peak Acceleration Calculations

Accelerometer $E_c = 7\sqrt{2}$ mv/g peak reading

Input lead and Amplifier Attenuation $A_i = 1 - \frac{300+100}{300+230} = 24.5\%$

Filter Attenuation $A_f = 3.5$ db or 33.2%

Standardized Accelerometer Voltage

$$E_s = E_a(1-A_i)(1-A_f)$$

The peak acceleration a_p is calculated from the following equation:

$$a_p = \frac{G_v d_o}{E_s} G_i$$

where d_o is the oscilloscope deflection (cm)

G_v is the Vertical Gain (mv/cm)

G_i is the Input Amplifier Gain

B. Initial Problems and Solutions

In order to obtain reproducible impact test results, several restrictions are automatically placed on the design of such a machine. Three of the main limitations (besides being able to withstand its own shocks) are:

(a) The acceleration-time pulse should be reproducible, and not vary over the carriage face,

(b) The machine should deliver a single positive pulse*, rather than a pulse disturbed by and followed by large amplitude carriage vibrations or rebound[2],

(c) The laboratory simulation of actual shock conditions must be adequately duplicated[3].

To meet these specifications, many changes in the mechanical construction were made and a electrical low pass filter was added

---

* A single positive pulse is the desired end since rebound of the carriage or negative pulses are very hard to reproduce consistantly.

to the electrical instrumentation circuit to eliminate three undesirable effects discussed previously. One of the initial shock pulses, illustrated in Figure 9a, was unintelligible, unreproducible and quite variable when measured across the carriage face. It was noted that during the carriage fall and after impact the steel guide wheels hitting the steel guide angles produced shock magnitudes greater than the expected drop shock. This effect was cancelled by using plywood or rubber wheels and lining the guides with rubber strips 1/8" thick.

Next, to insure a relatively free fall, the guide angles were plumbed and braced at the top. (Figure 1) This eliminated excessive machine vibrations, but did not reduce the hash in the shock pattern.

Finally a cast iron lathe face plate attached directly to the impact block holder replaced an existing 1/4" plate and four substructure supporting angles. Due to the extreme stiffness of the ribbed plate, the carriage vibrations were reduced to a minimum and the variation in acceleration on the plate eliminated. Figure 9b represents the shock pattern with these mechanical changes.

A further reduction of hash was achieved by using a low pass filter. (Figure 9c) It should be noted here that many of the high frequency components of the original signal are magnified out of proportion to their actual value because of the rising output of the accelerometer beyond 2500 cps.

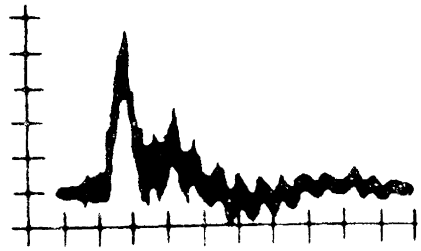

Peak Acceleration 90 g
Sweep 2.0 ms/cm

Figure 9a. Initial Shock Pulse

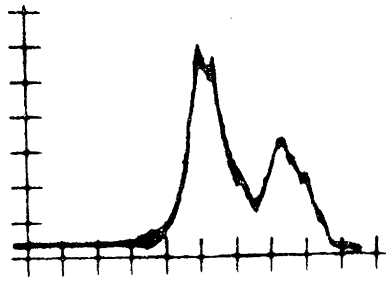

Peak Acceleration 80 g
Sweep 1.5 ms/cm

Figure 9b. Shock Pulse after Mechanical Design Changes

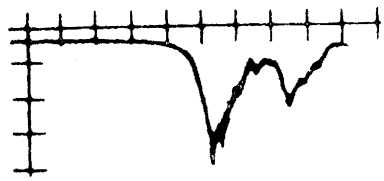

Peak Acceleration 80 g
Sweep 1.5 ms/cm

Figure 9c. Final Shock Pulse with Electrical Filter

Note: Figure 9c is inverted since it was taken with the dual trace oscilloscope along with Figure 9b.

C. Test Procedure and Dropping Technique

To obtain constant test conditions for reproducible results the following order of procedure is exercised in preparation for dropping:

1 The equipment leads are connected, starting with the accelerometer to the oscilloscope, insuring firm connections and a good electrical ground.

2 The equipment is turned on and allowed to warm up for 20 minutes.

3 During this time,

(a) The blocks for the test are bolted to the carriage mounting frame in such a way that the blocks hit on their long narrow side.

(b) The carriage is dropped a few times to compact the sand to the degree which will be experienced during the actual test.

(c) The sand is leveled by means of a block jig constructed to level the sand to the same height each time. Any excess sand is removed or if sand must be added #3b must be repeated again.

(d) The trigger mechanism is raised or lowered on the guide angle to trigger the sweep an instant before impact.

4 The Impact Amplifier Switches are set

(a) Gain - 1

(b) Capacitance Decade - 10 mmfd

(c) Imput Switch - Position 1

5 The Oscilloscope Controls are set

(a) Triggering Mode - DC

(b) Trigger Slope - External Negative

(c) Trigger Input - Negative battery lead to input other lead to ground

(d) Trigger Level - Slightly Negative

(e) Stability - Rotate clockwise to obtain a beam trace when the trigger is operated

(f) Time/cm - Variable, 1 ms/cm usually

(g) Multiplier - Variable, 1, 2, 2.5, 5 usually

(h) Horizontal Position and Vernier

Focus

Intensity

Astigmatism

Scale Illumination - Adjusted to give desired trace

6 The Plug-in Preamplifier Controls are set

(a) Input Selector - AC

(b) Volts/cm - Give maximum gain and retain trace on graticule

(c) Variable - Rotated fully clockwise

(d) Vertical Position - Trace bottom line of the graticule

7 Record Horizontal Sweep (5f), Multiplier (5g) and Vertical Gain (6b) Dial Settings.

Having followed this procedure the carriage is ready for raising to the test drop height and release. The solenoid release button when pressed should be held closed until the beam has traced the screen to prevent a visual transient from the release from disturbing the trace.

If a camera is used to record the trace, either a calibration wave must be used or the graticule illuminated to determine the shock magnitude. The camera shutter should be opened manually before the drop and closed immediately after the impact to prevent over-exposure due to the long persistent screen.

D. Shock Machine Calibration

1. Standard Pulses

The calibration curves for the shock machine using 2, 3, 4 and 6 sets of standard blocks (Figure 10b) were obtained by dropping the carriage from various heights and determining the peak acceleration from oscilloscope deflections. Initially three blocks were tested in

carriage positions 1, 4 and 7 (Figure 10a). For two blocks, block 4 was removed. Then positions 2 and 6 were filled for the four block test and the positions 3 and 5 for the 6 block test. This order of positioning was done to provide a wide base for impacts to prevent rocking of the carriage. After each drop the sand was always leveled for the next drop.

Figure 11 shows the calibration curves for each set of blocks and Figure 12 gives the characteristic pulse shape and pulse duration for these sets. These tests were conducted using a 30# dead load on the carriage.

2. Various Pulse Shapes

In order to obtain different shaped pulses three combinations of the blocks represented in Figure 10 were used. A step pulse shock was obtained by using 3V blocks (Figure 10c) mounted in positions 2, 4 and 6 with 2 standard blocks mounted in positions 3 and 5. This pulse is represented in Figure 13. The pulse using these V blocks alone was not different from the standard pulses. Figure 14 illustrates a square pulse produced by using two standard blocks mounted in positions 2 and 6 and one sharp V block (Figure 15d) in position 4. These sharp V blocks alone produced the triangular shaped pulse represented in Figure 15.

Block Arrangements and Shapes

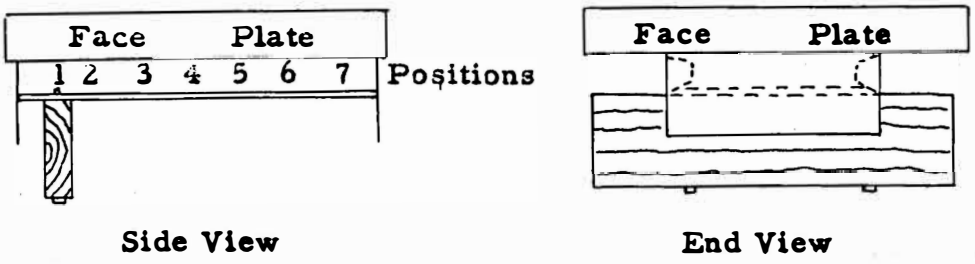

Side View End View

Figure 10a. Impact Block Mounting Details

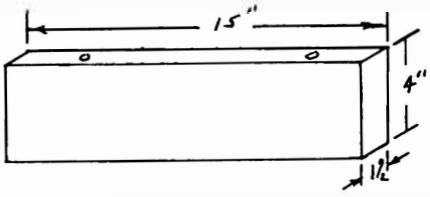

Figure 10b. Standard Impact Block

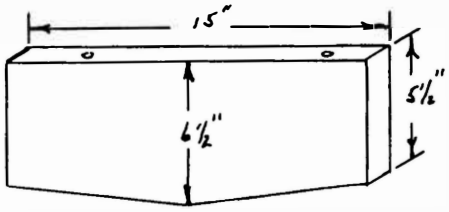

Figure 10c. V Block

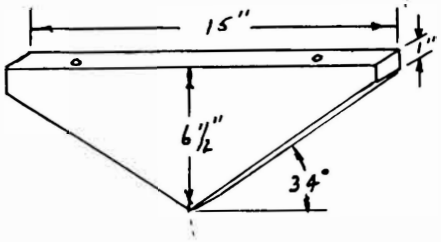

Figure 10d. Sharp V Block

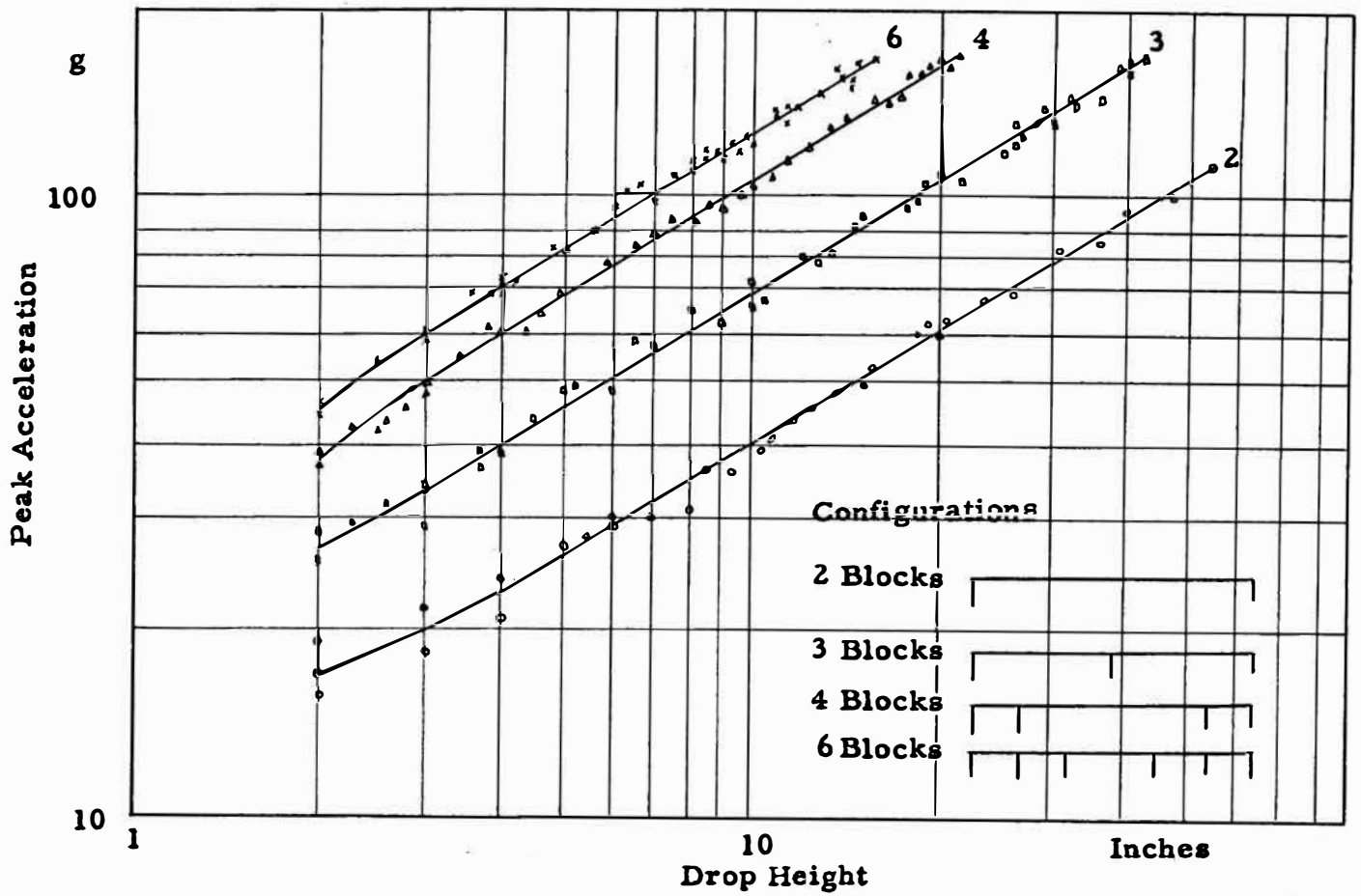

Figure 11. Calibration Curves for Standard Blocks

Characteristic Pulse Shapes

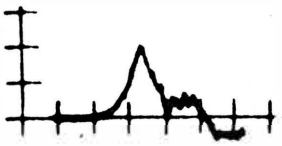

Peak Acceleration	44 g
Drop Height	12 in.
Sweep	2.5 ms/cm
Vertical Gain	0.1 v/cm

Figure 12a. Two Impact Blocks

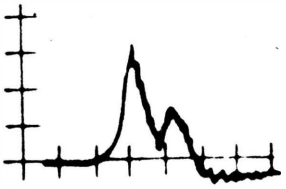

Peak Acceleration	68 g
Drop Height	10 in.
Sweep	2.5 ms/cm
Vertical Gain	0.1 v/cm

Figure 12b. Three Impact Blocks

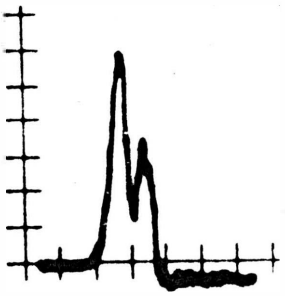

Peak Acceleration	120 g
Drop Height	12 in.
Sweep	2 ms/cm
Vertical Gain	0.1 v/cm

Figure 12c. Four Impact Blocks

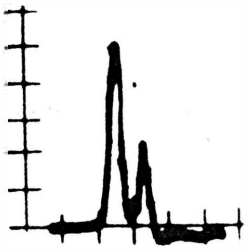

Peak Acceleration	160 g
Drop Height	13 in.
Sweep	2 ms/cm
Vertical Gain	0.15 v/cm

Figure 12d. Six Impact Blocks

Figure 13. Step Pulse

Peak Acceleration	68 g
Step Acceleration	36 g
Sweep	2.5 ms/cm
Vertical Gain	0.1 v/cm

(3 V Blocks 2 Standard)

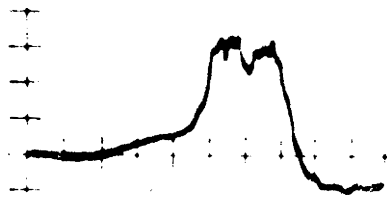

Figure 14. Square Pulse

Peak Acceleration	68 g
Sweep	2.5 ms/cm
Vertical Gain	0.1 v/cm

(1 Sharp V Block 2 Standard)

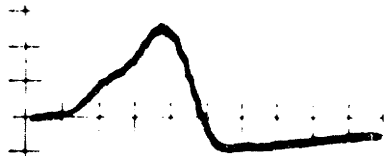

Figure 15. Triangular Pulse

Peak Acceleration	60 g
Sweep	2.5 ms/cm
Vertical Gain	0.1 v/cm

(3 Sharp V Blocks)

E. Solution of a Typical Impulse Vibration Problem

To illustrate the use of a drop tester a simple spring-mass system was subjected to an acceleration pulse. In this example, the acceleration pulse applied to the base of the spring-mass system was picked up by an accelerometer mounted on the yoke directly above the spring. Figure 16 shows this pulse and Figure 17 the spring-mass response which was picked up by an accelerometer mounted on the mass. (Figure 2)

The solution of this problem was obtained by using the Laplace Transform Method to solve the differential equation of motion for the system shown in Figure 18. The natural damped frequency and viscous damping constant were calculated from the acceleration versus time oscilloscope trace of the spring-mass system response. (Figure 17)

Peak Acceleration	40 g
Drop Height	2.5 in.
Sweep	0.25 ms/cm
Vertical Gain	50 mv/cm

Figure 16.
Pulse Applied to the System Base

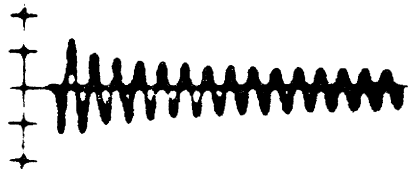

Sweep	100 ms/cm
Vertical Gain	50 mv/cm

Figure 17.
Spring Mass System Response

Laplace Transform Solution

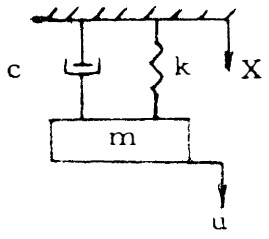

$y = u - X$

Figure 18. Spring Mass System

For this system the following constants were determined:

$m = 5.5/g$ slugs

$k = 1/74 \times 10^{-3}$ #/in.

$f_n = \omega_n/2\pi = 15.5$ c/sec.

ω_n = 97.4 rad./sec.

δ = 0.0602 #sec./in.

fnd = nd/2n = 15.42 c/s

ω nd = 96 rad./s

c_c = 2.76 #sec./in.

c = 0.0291 #sec./in.

r = 0.0105

By using an idealized pulse (Figure 19) the differential equation of motion:

$$mD^2u + cDy + ky = 0$$

may be set up and simplified into

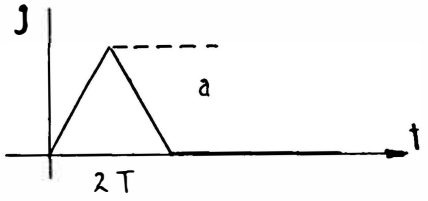

Figure 19. Idealized Pulse

$$D^2y + 2r\omega_n Dy + \omega^2_n y = -D^2X = a(t) = \wedge$$

Setting up the shock pulse in terms of a, T, t and Laplace step functions:

$$\wedge = a/T \left\{ t \left[S(o_1 t) - S(t-T) \right] + (2T-t) \left[S(t-T) - S(t-2T) \right] \right\}$$

and transforming the total equation with the Initial Conditions that when t = 0, yo = 0

$\dot{y}_o = 0$, the transformed equation becomes

$$(S^2 + 2r\omega_n S + \omega_n^2)y = \frac{a}{T} \frac{1}{S^2} (1 - 2e^{-TS} + e^{-2TS})$$

$$\mathcal{L}^{-1} \left[\frac{T}{a} y(s) = \frac{1}{S^2} \times \frac{1}{S^2 + 2r\omega_n S + \omega_n^2} \times (1 - 2e^{-TS} + e^{-2TS}) \right]$$

with certain mathematical simplifications the equation is now inverted and the solution becomes:

$$\omega_n^2 \frac{T}{a} y(t) = t - \frac{2r}{n} + \frac{\sqrt{8r^2+1}}{\omega_{nd}} \cos(\omega_{nd}t - \varphi)\, e^{-r\omega_{nd}t}$$

$$+ S(t-T)\left\{-2(t-T) + \frac{4r}{\omega_n} - \frac{2\sqrt{8r^2+1}}{\omega_{nd}} \cos(\omega_{nd}(t-2T) - \varphi)\, e^{-r\,\omega_{nd}(t-T)}\right\}$$

$$+ S(t-2T)\left\{(t-2T) - \frac{2r}{\omega_n} - \frac{\sqrt{8r^2+1}}{\omega_{nd}} \cos(\omega_{nd}(t-2T) - \varphi)\, e^{-r\omega_{nd}(t-2T)}\right\}$$

$$\text{where } S(t-T) = \begin{cases} 0 \text{ for } t < T \\ 1 \text{ for } t \geq T \end{cases}$$

$$\text{and } S(t-2T) = \begin{cases} 0 \text{ for } t < 2T \\ 1 \text{ for } t \geq 2T \end{cases}$$

$$\varphi = \tan^{-1} \frac{\omega_n(r^2+1)}{2r\omega_{nd}}$$

A plot of the second derivative of y(t) with respect to time of this solution is given in Figure 20, and is compared with the oscilloscope trace plotted to the same scale.

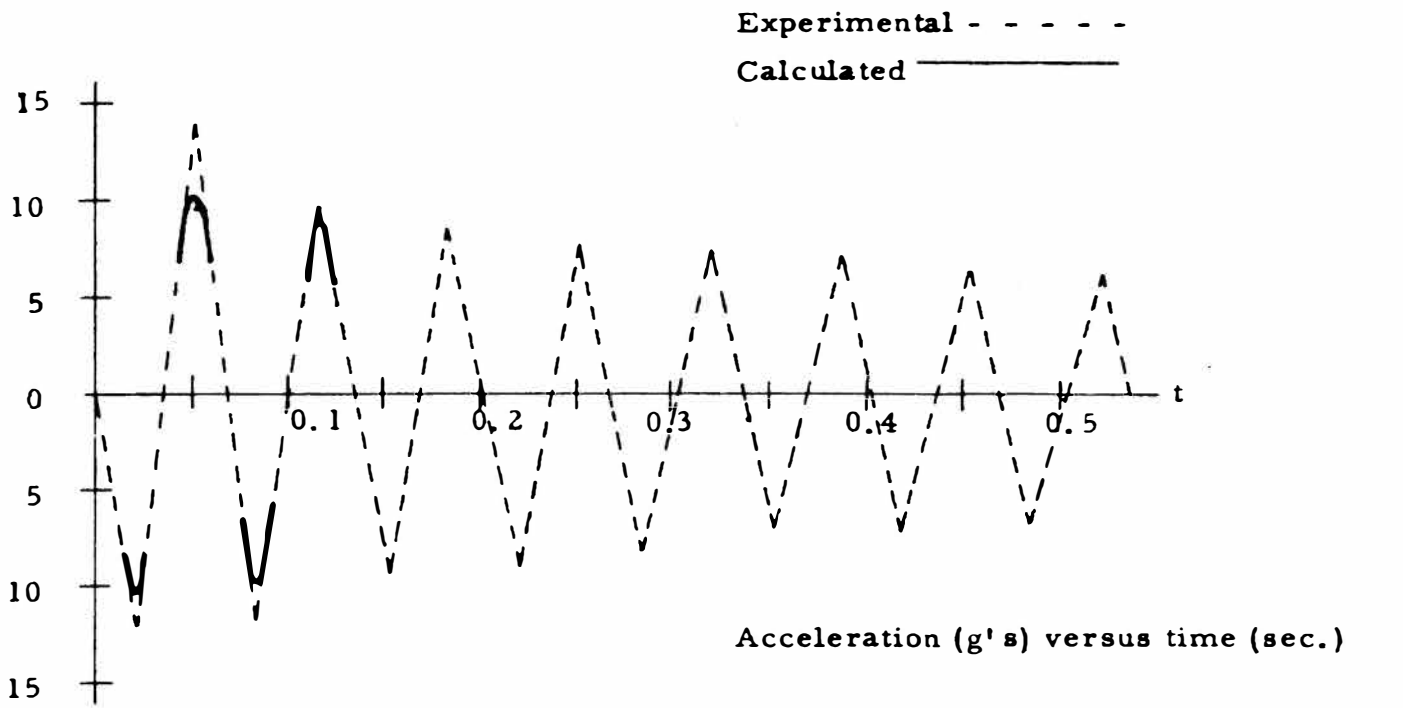

Figure 20. Plot of Spring Mass System Response - Experimental and Calculated

VI. DISCUSSION OF RESULTS

A. Calibration Curves

The calibration curves have a maximum deviation of ± 15% in the useful range which is fully adequate for practical work[10]. It may be seen that for low height drops there are great variations in peak accelerations. Many factors influence this, but mainly the inability (1) to compact the sand uniformly to a constant density for each drop and (2) to achieve a perfectly flat impact each time.

One effect noted is that for low drops the curves for 2 and 3 blocks tend to rise slightly and the curves for 4 and 6 blocks tend to droop, although not as noticeably as the former. The reason for this is that for high drops of 2 and 3 blocks tend to loosen the sand more than lower drops, thus producing a more compact sand pit and therefore higher accelerations for low drops. The reverse effect happens for 4 and 6 blocks. Low drops produce a more compact sand pit than high ones.

Due to the weight of the carriage, peak accelerations lower than 20 g's could not be obtained using these blocks.

B. Pulse Shapes

As can be seen by Figures 13, 14 and 15, the desired effect of obtaining distinctively different pulse shapes was achieved. Exact

prediction of the pulse shape before testing a block combination was not considered in this thesis. The reproductibility of these pulse shapes for any given combination is very good after two or three drops have been made using this combination. The reason for this is that after a few drops the sand compactness is not altered from then on. It may be noted from the pulses that a negative pulse is produced probably due to the penetration of the V blocks into the sand.

C. Impulse Vibration Test

A plot of the experimental response with that of the calculated response (Figure 20) are very similar except for the first period after which they are essentially coincident. This discrepancy was caused either by the spring being stretched beyond its linear range or the slight rebound of the carriage not considered in the solution of the problem.

D. Recommendations

It is believed that more consistant and reproducible shock pulses will be obtained if the following two conditions are met:

(1) The machine base which is presently bolted to a concrete floor should be set on a firmer foundation and grouted in place.

(2) The box frame which supports the carriage face plate should either be stiffened and made as to support the center of the plate or be removed and the impact blocks attached directly to the plate.

With these changes the maximum potentiality of this drop tester will be achieved.

VII. SUMMARY AND CONCLUSIONS

In this thesis, the problems of building, instrumenting and testing a shock machine are presented and discussed.

The machine was calibrated over a range of 30 to 175 g's with a 30# test load using standard impact blocks. Several different shaped blocks were tested which produced distinctively different pulse waves.

As an example of the application of a drop tester, a simple spring-mass system with internal damping was impulse tested and the differential equation of motion was solved by means of the Laplace Transform.

In general the range of peak acceleration is great enough to accommodate most laboratory applications. By using various combinations of different shaped blocks several impulse shapes may be obtained. Determination of complex transient vibrations resulting from varied shock pulses is easily solved by the Laplace Transform Method. The number of calculations with this method of solution does not increase as fast with the complexity of shock pulse as other methods.

VIII. ACKNOWLEDGEMENTS

The author expresses his sincere appreciation to all the members of the Department of Applied Mechanics at Virginia Polytechnic Institute, for their aid and advice and making the author's year of graduate study a pleasurable and a profitable one.

The writer is deeply indebted to Professor F. J. Maher, for his patient consideration and guidance on this thesis and throughout this year.

To Doctor N. J. Huffington, the writer expresses his thanks for providing help and technical advice throughout the progress of this thesis.

To C. K. McCauley, Applied Mechanics Laboratory Technician and Mrs. Marilyn Brna, typist, the writer extends thanks for their aid and encouragement in making this thesis possible.

IX. APPENDIX

A. Electrical Circuit Elements

The electrical circuit elements used in this thesis are:

1. Accelerometer — Model No. 2610, Serial No. 306
2. Input Amplifier — Model No. 2614, Serial No. 108
3. Power Supply — Model No. 2610

   Endevco Corporation
   180E California Street
   Pasadena, California
4. Oscilloscope — Type 531, Serial No. 899
5. Plug-in Preamplifiers — Type 53B Wide Band High Gain, Serial No. 1051; Type 53C Dual Trace, Serial No. 2116

   Textronix
   Portland 7, Oregon
6. Vacuum Tube Voltmeters — Model No. 400C, Serial No. 11136; Model No. 400C, Serial No. 11164
7. Audio Oscillator — Model No. 200B

   Hewett-Packard Company
   Palo Alto, California

B. Sand Grain Distribution Test Data

Grain Shape - Sub Angular

Sieve Number	Percentage
20	37.3
30	18.3
40	15.5
50	13.1
70	8.2
100	3.7
140	1.1
200	0.6
270	0.1
Pan	0.5
	98.4
Airborn dust*	1.6
Total	100.0%

* Due to the percentage of Airborn dust, test periods must not exceed thirty minutes duration for danger of silicosis

X. BIBLIOGRAPHY

Books and Papers

1. Macduff, J. N. and Currier, J. R.: "Vibration Control" McGraw Hill Book Company, Inc., New York, 1958.
2. Kornhauser, M.: Potentialities of the Impact Machine for Producing High Accelerations, Proc. SESA, Vol. XIV, No. 2, 1957.
3. Armstrong, J. H.: Shock Testing at the Naval Ordnance Laboratory, Proc. SESA, Vol. XI, No. 1, 1948.
4. Vigness, Irwin: Some Characteristics of Navy "High Impact" Type Shock Machines, Proc. SESA, Vol. V, No. 1, 1947.
5. Fischer, E. G.: Lateral Vibrations and Stress in a Beam Under Shock Machine Loading, Proc. SESA, Vol. V, No. 1, 1947.
6. Welch, W. P.: A Proposed New Shock Measuring Instrument, Proc. SESA, Vol. V, No. 1, 1947.
7. Salvadori, M. G.: A Mathematical Treatment of the Generalized Hertz Impact of a Mass on a Simply Supported Beam, The Welding Journal, Vol. 26, No. 7, July 1947.
8. Huter, T. F. and Bolt, R. H.: "Sonics" John Wiley and Sons, Inc., New York, 1955.
9. Everitt, W. L. and Anner, G. E.: "Communication Engineering" McGraw Hill Book Company, Inc., New York, 1958.

Bulletins and Instruction Manuals

10. Berry Product Bulletin 535: Component Shock Machine
Berry Corporation
Watertown, Massachusetts, 1953.

11. Endevco Instrument Manual: Instruction Manual and Calibration Chart for Accelerometers and Input Amplifiers, Endevco Corporation
Pasadena, California.

The vita has been removed from the scanned document